Acoustooptic figure of merit of Tl_3AsS_4 crystals. The case of acoustic waves propagation along crystallographic axes

[1] Mys O., [1] Kryvyy T., [2] Mytsyk B. and [1] Vlokh R.

[1] Vlokh Institute of Physical Optics, 23 Dragomanov Street, 79005 Lviv, Ukraine, vlokh@ifo.lviv.ua
[2] N. V. Karpenko Physico-Mechanical Institute, 5 Naukova Street, 79601 Lviv, Ukraine

Received: 19.02.2018

Abstract. We analyze isotropic and anisotropic acoustooptic interactions in Tl_3AsS_4 crystals in the principal crystallographic planes under the condition that the optical and acoustic waves propagate close to the crystallographic axes. We find that the maximal acoustooptic figures of merit are equal to 2181×10^{-15} s^3/kg and 1990×10^{-15} s^3/kg for the cases of isotropic and anisotropic diffractions, respectively.

Keywords: acoustooptic figure of merit, anisotropy, fangite minerals, Tl_3AsS_4 crystals

PACS: 42.70.Nq, 42.25.Fx
UDC: 535.42

1. Introduction

Thallium arsenic sulfosalt crystals, Tl_3AsS_4, are representatives of a family of fangite minerals [1]. They belong to the point symmetry group *mmm* under normal conditions. Their unit-cell parameters are equal to $a = 8.98$ Å, $b = 10.8$ Å and $c = 8.86$ Å [2, 3] (i.e., we have the inequality $c < a < b$ [4]) and the unit cell contains four formula units ($Z = 4$) [5]. Tl_3AsS_4 is transparent in a long-wavelength part of the visible spectral range and in a wide part of the infrared range (from 0.6 to 12 μm) [2]. The crystal is optically biaxial and has the refractive indices $n_a = 2.829$, $n_b = 2.774$ and $n_c = 2.825$ at the light wavelength $\lambda = 632.8$ nm [2]. The acute angle between the optic axes determined experimentally is equal to 28.46 ± 0.1 deg at the same wavelength, which agrees well with the angle 29.76 deg calculated basing on the refractive indices [2].

Thallium arsenic sulfosalt is interesting from the viewpoint of its applications in the working cells of acoustooptic (AO) devices. It has been efficiently used in tunable AO filters for the far infrared range. Moreover, Tl_3AsS_4 is a promising material for thermal imaging [6]. Recently, we have determined the complete matrices of piezooptic and elastooptic coefficients (EOCs) [7] for the Tl_3AsS_4 crystals, together with the complete matrices of elastic stiffness and compliance coefficients [8]. It has been found that the piezooptic coefficients are very high, being 10^{-11} N/m^2 in the order of magnitude. This implies that Tl_3AsS_4 can be regarded as one of the best piezooptic materials. The same concerns the EOCs, of which modules belong to the region of 0.28–0.54. We have also shown [8] that the anisotropic and isotropic AO interactions of light with the slowest transverse ($v_{32} = v_{23} = 630$ m/s) and longitudinal ($v = 2077$ m/s) acoustic waves result in extremely high AO figures of merit (AOFMs), respectively 1.99×10^{-12} s^3/kg and 9.45×10^{-13} s^3/kg. These facts allow one to consider the Tl_3AsS_4 crystals as one of the best AO materials for the visible and infrared ranges.

Notice that the other geometries of AO interactions, even those at which the acoustic waves propagate along the principal crystallographic axes, have not yet been scrutinized. The only exception is the work [2] where the absolute values of several EOCs and the corresponding AOFMs have been determined for the case of isotropic diffraction. These parameters are respectively equal to $p_{31} \simeq 0.27$, $p_{32} \simeq 0.32$ and $p_{33} \simeq 0.39$ (at $\lambda = 632.8$ nm), and 453×10^{-15} s^3/kg, 555.7×10^{-15} s^3/kg and 792.8×10^{-15} s^3/kg. The above AOFMs have been determined under the conditions of isotropic interactions of the optical waves polarized along the crystallographic axis *c* with the longitudinal acoustic waves propagating along the crystallographic axes. It would be worthwhile to remind in this respect that the velocity of the quasi-longitudinal wave does not manifest essential anisotropy, varying from 2077 to 2369 m/s [7]. On the other hand, the so-called principal EOCs lie in the region 0.28–0.54 and so can change almost twice. Hence, the AOFM can sufficiently differ for different interaction geometries, even in the simplest case of isotropic diffraction at the quasi-longitudinal wave. In addition, the efficiency of the anisotropic AO diffraction can vary within the crystallographic planes. In the present work we analyze anisotropy of the AOFM in Tl_3AsS_4 for the cases when the acoustic waves propagate close to the crystallographic axes and the interaction planes coincide with the crystallographic planes.

2. Results and discussion

Let us consider the isotropic AO diffraction at the longitudinal acoustic waves. We have analyzed searately the three crystallographic planes, which represent now the planes of AO interactions. As menioned before, the incident and diffracted optical waves propagate close by the crystallographic axes, while the acoustic wave propagates along one of these axes. Taking the optical birefringence into account, one can consider four types of isotropic interactions for each of the interaction planes.

Let us start with the crystallographic plane *ab*. As seen from Fig. 1a, four types of interactions can be realized in this case under the conditions mentioned above. Two of them correspond to diffractions at the acoustic wave propagating along the *b* axis (i.e., the types (1) and (2)) and the other two, the types (3) and (4), refer to the acoustic wave propagating along the *a* axis. The most efficient is the interaction geometry (2) when the longitudinal acoustic wave propagates along the *b* axis, while the incident and diffracted optical waves propagate close to the *a* axis, being polarized parallel to the *b* axis. Then the AOFM, which is determined as $M_2 = n^6 p_{ef}^2 / \rho v_{ij}^3$ (with *n* being the refractive index, p_{ef} the effective EOC, v_{ij} the acoustic wave velocity, ρ the material density, and *i* and *j* denoting the directions of propagation and polarization, respectively), is extremely high. As seen from Table 1, it reaches the value $M_2 = 2181 \times 10^{-15}$ s^3/kg. This AOFM is achieved due to large magnitude of the appropriate EOC. The type (3) of the interactions is also very efficient (see Fig. 1a and Table 1), with the AOFM amounting to 1374×10^{-15} s^3/kg.

Now we consider the interaction plane *bc*. Here the most efficient are the AO interactions of the type (4), with the AOFM being equal to 2181×10^{-15} s^3/kg (see Fig. 1b). It is almost the same interactions as those of the type (2) in the plane *ab*, with the only difference that the optical waves propagate close to the *a* axis in the plane *ab* in the former case and close to the *c* axis in the plane *bc* in the latter case. The interaction types (1), (2) and (4) are the most efficient in the *ac* interaction plane (see Fig. 1c). In particular, the type (1) is characterized by the AOFM equal to 1374×10^{-15} s^3/kg. As seen from Table 1, only a slightly lower AOFM,

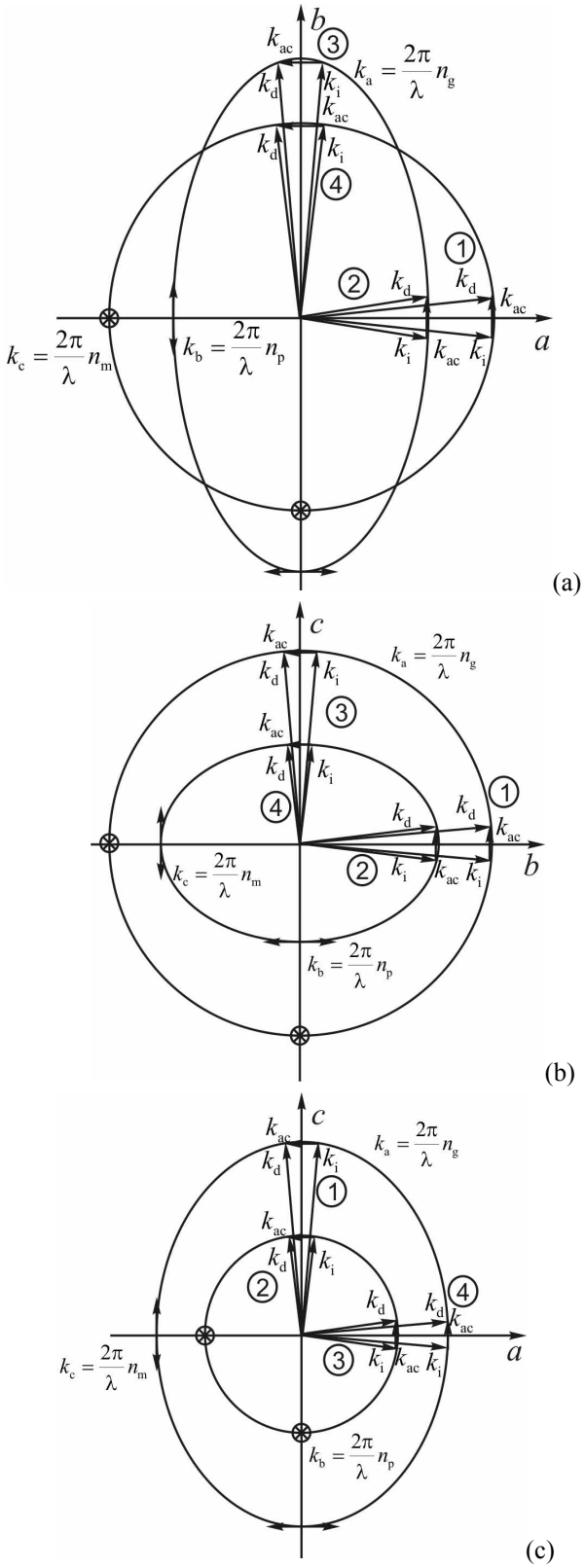

Fig. 1. Isotropic AO diffraction in crystallographic planes *ab* (a), *bc* (b) and *ac* (c).

Table 1. Constitutive parameters and AOFMs of Tl_3AsS_4 calculated for the case of isotropic diffraction at $\lambda = 632.8$ nm .*

		Type of interaction			
		(1)	(2)	(3)	(4)
Interaction plane *ab*	Effective EOC (p) and refractive index (n)	p_{32}=0.28, p_{32}=0.32** n_3=2.825	p_{22}=0.54, n_2=2.774	p_{11}=0.44, n_1=2.829	p_{31}=0.28, p_{31}=0.27** n_3=2.825
	Acoustic wave velocity, m/s	v_{22}=2142	v_{22}=2142	v_{11}=2267	v_{11}=2267
	M_2, 10^{-15} s^3/kg	654 555.7**	2181	1374	552 453**
Interaction plane *bc*	Effective EOC (p) and refractive index (n)	p_{13}=0.31, n_1=2.829	p_{33}=0.43, p_{33}=0.39** n_3=2.825	p_{12}=0.32, n_1=2.829	p_{22}=0.54, n_2=2.774
	Acoustic wave velocity, m/s	v_{33}=2829	v_{33}=2829	v_{22}=2142	v_{22}=2142
	M_2, 10^{-15} s^3/kg	598	1140 792.8**	861	2181
Interaction plane *ac*	Effective EOC (p) and refractive index (n)	p_{11}=0.44, n_1=2.829	p_{21}=0.45, n_2=2.774	p_{23}=0.36, n_2=2.774	p_{33}=0.43, p_{33}=0.39** n_3=2.825
	Acoustic wave velocity, m/s	v_{11}=2267	v_{11}=2267	v_{33}=2829	v_{33}=2829
	M_2, 10^{-15} s^3/kg	1374	1277	715	1140 792.8**

* EOC and acoustic-wave velocities are determined in our works [6, 7], whereas the refractive indices and the density (6200±40 kg/m^3) are taken from Ref. [2].
** EOCs and AOFM determined experimentally with the Dixon–Cohen technique [9, 10] in Ref. [2] are presented for comparison.

1277×10^{-15} s^3/kg and 1140×10^{-15} s^3/kg, are peculiar for the types (2) and (4), respectively. Again, these huge values are due to large magnitudes of the EOC. Thus, the maximal AOFM which can be reached in the case of AO interactions with the longitudinal acoustic wave in the crystal–logra–phic planes under the conditions mentioned above is equal to 2181×10^{-15} s^3/kg. In general, the AOFM values calculated by us agree fairly well with the parameters obtained experimentally using the Dixon–Cohen method [2]. The only difference is somewhat higher calculated values, if com–pared with the experimental ones. At the same time, the EOCs determined in Ref. [6] and Ref. [2] do not reveal such a correlation. We assume that the authors of the work [2] have not taken into account the light absorption and the internal reflection, when calculating the AOFMs and the EOCs. Nonetheless, the both parameters agree quite well if one accounts for the EOC errors.

Let us proceed with considering the anisotropic diffraction in Tl_3AsS_4, when the light interacts with the shear acoustic waves in the crystallographic planes. We assume for simplicity that the incident optical wave propagates along one of the crystallographic axes (see Fig. 2). Let the incident optical wave polarized parallel to the *b* axis propagates along the *a* axis, and the acoustic wave polarized parallel to the *c* axis propagates along the *b* axis in the interaction plane *ab*. Here we deal with the interaction type (1), i.e. the anisotropic diffraction occurs with appearance of the diffracted optical wave polarized along the *c* axis. As seen from Fig. 2a and Table 2, then the AOFM becomes very high (1990×10^{-15} s^3/kg). In case of the AO interaction type (2) and the same interaction plane, the acoustic wave propagates with the velocity $v_{13} = 1176$ m/s along the *a* axis, while the incident and diffracted optical waves have their polarizations parallel to the *c* and *a* axes, respectively. The AOFM for this case is equal only to 81×10^{-15} s^3/kg.

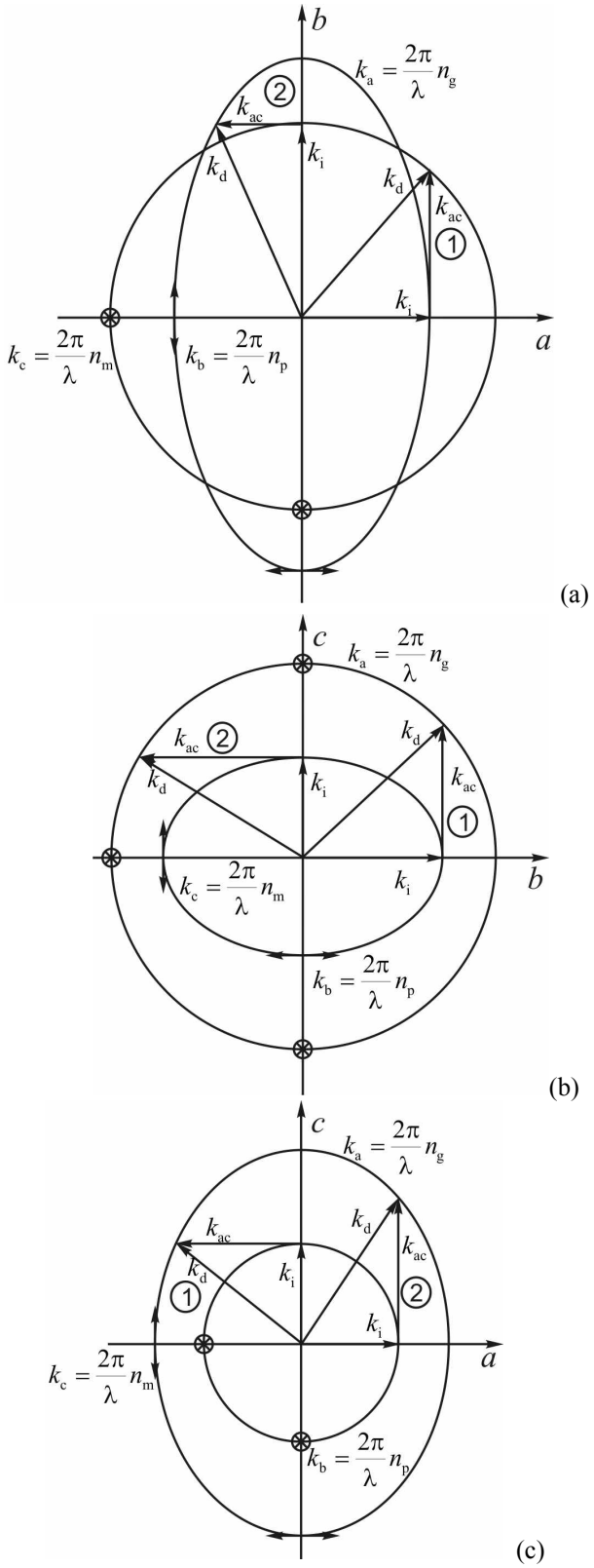

Fig. 2. Anisotropic AO diffraction in crystallographic planes *ab* (a), *bc* (b) and *ac* (c).

Table 2. Constitutive parameters and AOFMs of Tl_3AsS_4 calculated for the case of anisotropic diffraction at $\lambda = 632.8$ nm .

Interaction plane	*ab*		*bc*		*ac*	
Type of interaction	(1)	(2)	(1)	(2)	(1)	(2)
Effective EOC (p) and refractive indices (n)	p_{44}=0.08, n_2=2.774, n_3=2.825	p_{55}=0.04, n_1=2.829, n_3=2.825	p_{55}=0.04, n_1=2.829, n_3=2.825	p_{66}≈0.00, n_1=2.829, n_2=2.774	p_{66}≈0.00, n_1=2.829, n_2=2.774	p_{44}=0.08, n_2=2.774, n_3=2.825
Acoustic wave velocity, m/s	v_{23}=630	v_{13}=1176	v_{31}=1176	v_{21}=1196	v_{21}=1196	v_{32}=630
M_2, 10^{-15} s^3/kg	1990	81	81	~ 0	~ 0	1990

Let us consider the AO interaction type (1) and the interaction plane *bc*. Then the anisotropic diffraction is possible for the case of interactions with the acoustic wave, of which velocity is equal to $v_{31} = 1176$ m/s. The corresponding AOFM amounts to 81×10^{-15} s^3/kg. The AOFM is close to zero in case of the interaction type (2) and the same interaction plane, since the appropriate effective EOC is very small ($p_{66} = 0.00\pm0.03$). For the same reason the AOFM is also close to zero for the AO interactions of the type (1) in the plane *ac*. However, the AOFM becomes very high, 1990×10^{-15} s^3/kg, in case of the interaction type (3) (see Fig. 2c). Finally, we stress that the collinear AO diffraction cannot be implemented whenever the optical and acoustic waves propagate along the crystallographic axes. This is caused by the fact that the corresponding EOCs p_{54}, p_{56}, p_{64}, p_{65}, p_{64}, p_{46} and p_{45} are equal to zero for the crystals of the symmetry group *mmm*.

3. Conclusions

In the present work we have analyzed both the isotropic and anisotropic AO interactions in the Tl_3AsS_4 crystals. The additional conditions include the AO interactions in the crystallographic planes and propagation of the optical and acoustic waves close by the crystallographic axes. We have found that the maximal AOFM value is equal to 2181×10^{-15} s^3/kg in case of the isotropic diffraction. This AOFM can be reached for the following two interaction geometries: (i) the AO interaction occurs in the crystallographic plane *ab*; the longitudinal acoustic wave propagates along the *b* axis, while the incident and diffracted optical waves polarized along the *b* axis propagate close to the *a* axis; (ii) the AO interaction occurs in the crystallographic plane *bc*; the longitudinal acoustic wave propagates along the *b* axis, and the optical waves polarized along the *b* axis propagate close to the *c* axis.

The maximal AOFM for the case of anisotropic diffraction is equal to 1990×10^{-15} s^3/kg. It is reached for the following two interaction geometries: (i) the AO interaction occurs in the *ab* plane; the incident wave polarized parallel to the *b* axis propagates along the *a* axis, while the acoustic wave polarized parallel to the *c* axis propagates along the *b* axis, with appearance of the diffracted optical wave polarized along the *c* axis; (ii) the AO interaction occurs in the *ac* plane; the acoustic wave polarized parallel to the *b* axis propagates along the *c* axis, while the incident optical wave polarized parallel to the *b* axis propagates along the *a* axis, with appearance of the diffracted wave polarized parallel to the *c* axis.

Acknowledgement

The authors acknowledge the Ministry of Education and Science of Ukraine for financial support of the present study (the Projects #0117U000802 and #0118U003899).

References

1. Wilson J R, Sen Gupta P K, Robinson P D and Criddle A J, 1993. Fangite, Tl3AsS4, a new thallium arsenic sulfosalt from the Mercur Au deposit, Utah, and revised optical data for gillulyite. Amer. Mineral. **78**: 1096–1103.
2. Roland G W, Gottlieb M and Feichtner J D, 1972. Optoacoustic properties of thallium arsenic sulphide, Tl_3AsS_4. Appl. Phys. Lett. **21**: 52–54.
3. Goutzoulis A, Gottlieb M, Davies K and Kun Z, 1985. Thallium arsenic sulfide acoustooptic Bragg cells. Appl. Opt. **24**: 4183–4188.
4. ANSI/IEEE Std 176-1987, IEEE Standard on Piezoelectricity 1987 American National Standards Institute The Institute of Electrical and Electronics Engineers, Inc, New York, USA.
5. Anthony J. W., Bideaux R A, Bladh K W, and Nichols M C, Eds., Handbook of mineralogy. Mineralogical Society of America, Chantilly, VA 20151-1110, USA. http://www.handbookofmineralogy.org/.
6. Denes L J, High performance cameras for hyperspectral and polarimetric imaging research, Technical Report (Carnegie Mellon University, 2003) (http://repository.cmu.edu/robotics/697/).
7. Mytsyk B, Kryvyy T, Demyanyshyn N, Mys O, Martynyuk-Lototska I, Kokhan O and Vlokh R, 2018. Piezo-, elasto- and acousto-optic properties of Tl_3AsS_4 crystals. Appl. Opt. **57**: 3796–3801.
8. Martynyuk-Lototska I, Kushnirevych M, Zapeka B, Krupych O, Kokhan O, Pogodin A, Peresh E, Mys O and Vlokh R, 2015. Acoustic anisotropy of acoustooptic Tl_3AsS_4 crystals. Appl. Opt. **54**: 1302–1308.
9. Dixon R W and Cohen M G, 1966. A new technique for measuring magnitudes of photoelastic tensor and its application to lithium niobate. Appl. Phys. Lett. **8**: 205–207.
10. Dixon R W, 1967. Photoelastic properties of selected materials and their relevance for applications to acoustic light modulators and scanners. J. Appl. Phys. **38**: 5149–5152.

Mys O., Kryvyy T., Mytsyk B. and Vlokh R. 2018. Acoustooptic figure of merit of Tl_3AsS_4 crystals. The case of acoustic waves propagation along crystallographic axes. Ukr.J.Phys.Opt. **19**: 99 – 105

Анотація. *Проаналізовано ізотропну та анізотропну акустооптичні взаємодії в кристалах Tl_3AsS_4 у кристалографічних площинах за умови, що оптичні і акустичні хвилі поширюються в напрямках, близьких до кристалографічних осей. Виявлено, що для ізотропної та анізотропної дифракції максимальні значення коефіцієнта акустооптичної якості дорівнюють відповідно 2181×10^{-15} с^3/кг і 1990×10^{-15} с^3/кг.*